

An actinometric study of C₂H₂ plasma polymerization and film properties

Rogério Pinto Mota, Tadashi Shiosawa, Steven Frederick Durrant, and Mário Antônio Bica de Moraes

Citation: *Journal of Vacuum Science & Technology A* **13**, 2747 (1995); doi: 10.1116/1.579699

View online: <http://dx.doi.org/10.1116/1.579699>

View Table of Contents: <http://scitation.aip.org/content/avs/journal/jvsta/13/6?ver=pdfcov>

Published by the AVS: Science & Technology of Materials, Interfaces, and Processing

Instruments for advanced science

Gas Analysis



- dynamic measurement of reaction gas streams
- catalysis and thermal analysis
- molecular beam studies
- dissolved species probes
- fermentation, environmental and ecological studies

Surface Science



- UHV TPD
- SIMS
- end point detection in ion beam etch
- elemental imaging - surface mapping

Plasma Diagnostics



- plasma source characterization
- etch and deposition process reaction kinetic studies
- analysis of neutral and radical species

Vacuum Analysis



- partial pressure measurement and control of process gases
- reactive sputter process control
- vacuum diagnostics
- vacuum coating process monitoring

contact Hiden Analytical for further details

HIDEN
ANALYTICAL

info@hideninc.com

www.HidenAnalytical.com

CLICK to view our product catalogue



An actinometric study of C₂H₂ plasma polymerization and film properties

Rogério Pinto Mota

*Departamento de Física e Química, Faculdade de Engenharia, UNESP, 12500-000 Guaratinguetá
São Paulo, Brazil*

Tadashi Shiosawa, Steven Frederick Durrant, and Mário Antônio Bica de Moraes

Instituto de Física Gleb Wataghin, UNICAMP, 13083-970 Campinas São Paulo, Brazil

(Received 28 April 1994; accepted 18 August 1995)

Thin polymer films were grown in radio frequency discharges containing C₂H₂. Actinometry revealed the trend in the plasma concentration of the CH species as a function of the operating pressure. The C–H bond density in the films, revealed by infrared analysis, was found to increase with the pressure of C₂H₂ in a similar way to that of the concentration of the CH species in the discharge. From transmission ultraviolet-visible spectroscopy data, optical parameters of the polymers, namely, the refractive index and the optical gap, were calculated. For the range of pressure studied, the refractive index decreased from 1.73 to 1.63 and the optical gap increased from 2.4 to 3.3 eV. Finally, measurements of the residual stress of the polymer films were carried out by the bending beam method, using a He–Ne laser, yielding values from 0.05 to 0.3 GPa. © 1995 American Vacuum Society.

I. INTRODUCTION

The plasma polymerization process began to attract academic and technological interest after some experiments were developed by Goodman,¹ who synthesized solid dielectric compounds using glow discharges of organic gases. At the present time, this type of process is of interest in the synthesis of new materials, particularly thin films exhibiting remarkable characteristics such as high uniformity, good adhesion to different substrates, and a lack of pinholes, as well as exhibiting singular optical, electrical, and mechanical properties. Such films have many promising applications as perm-selective membranes,^{2–5} anticorrosive surfaces,^{6–8} humidity sensors,⁹ temperature sensors,¹⁰ electrical resistors, and use in integrated circuit lithography,^{11–13} in integrated optics,¹⁴ and as windows and optical filters.¹⁵ Plasma polymerization is a well established technique but poorly understood because the plasma is very reactive and produces a large number of chemical species that form polymer films through chemical reactions whose mechanisms are very complex.¹⁶

On the other hand, despite progress in the technology of these polymers, we know little about their properties, such as mechanical stress,^{17,18} electrical,^{19–21} and optical properties²² as well as electronic bond structure.^{23,24}

In this article, we report on a study of the plasma process and the structural, optical, and mechanical properties of thin polymer films deposited by acetylene glow discharges. Optical emission spectroscopy was used to study the discharge environment. In particular, the actinometric technique was utilized to find trends in the concentrations of species present in the plasma which may play a role in the polymerization process.

The actinometric technique, which uses the emission from an inert probe gas (actinometer) to obtain relative concentrations of species of interest, is well established in current literature.^{25,26} This technique depends upon the fact that the excitation mechanisms of the species x and the actinometer a are predominantly by direct electron impact. In addition, the

excited states thus formed should decay only by photon emission. Finally, the threshold energies for both transitions should be the same. Actinometry relies on the fundamental relation²⁷

$$I_a = K_a N_a \eta_a, \quad (1)$$

where a refers to actinometer and I , N , and η are the intensity of emission, the concentration of the species in the ground state, and the excitation efficiency, respectively, and K is a constant. Thus, at a constant actinometer concentration of a few percent in the feed (which does not disturb the discharge), the concentration of the species of interest $[x]$ is related to the concentration of the actinometer $[a]$ by

$$[x]/[a] \propto I_x / I_a, \quad (2)$$

where I_x and I_a are the optical emission intensities of the species x and a , respectively.

The relative plasma CH concentration data were related to the C–H bond densities of the samples determined by transmission infrared reflection spectroscopy (IRS). By absorption ultraviolet-visible (UV-vis) spectroscopy some optical parameters, principally the refractive index and absorption coefficient, were also studied as a function of the deposition parameters. Residual stress measurements were also performed to investigate the role of intrinsic stress in the mechanical stability of the film.

II. EXPERIMENT

The experimental arrangement used was essentially the same as that described elsewhere.²⁸ Briefly, it consists of a Pyrex reactor of 7.5 cm internal diameter and 25.0 cm length, which opens into a bell-like structure 19.0 cm in diameter and 27.0 cm in height. Gases were fed to the reactor via needle valves and flowmeters (Datametrics, type 831).

TABLE I. Spectral data of species of interest.

Species	System	λ (nm)	Threshold energy (eV)
H	$2p^2P^0_{3/2}, 3d^2D_{3/2}$ $\frac{2}{2}$	656.3	12.09
CH	$A^2\Delta \cdot X^2\Pi$	431.4	<11
N ₂	$C^3\Pi_u \cdot B^3\Pi_g$	337.1	11.2
Ar	$4p^1(1/2) - 4s^1(1/2)$	750.3	13.47

The radio frequency (rf) generator (120 MHz, 40 W) was connected to ring electrodes through an impedance matching circuit and through-line wattmeter.

Acetylene and the actinometers (argon and nitrogen) were supplied from gas cylinders. The gases were of 99.98% minimum purity. A Pirani gauge, previously calibrated to nitrogen with the use of a capacitance manometer (Datametrics, Barcelona, type 600), was used for pressure indication.

The light from the plasma left the chamber via a quartz window and reached the slit of a 1-m-focal length monochromator (Spex Industries, model 14300). The output signal of the UV-vis photomultiplier was monitored on a chart recorder via an electrometer. Films for analysis by UV and infrared reflection spectroscopy (IRS) were prepared on quartz and KCl substrates, respectively. A UV-visible spectrophotometer (Perkin-Elmer, model Lambda 9) was used to obtain spectra and infrared analysis was performed using a Jasco (model IR 700) spectrophotometer. Film thickness was measured by an interferometric microscope (Varian, A-scope). The residual stress measurements were performed by the bending beam method,²⁹ using the apparatus described in a separate paper.³⁰

III. RESULTS AND DISCUSSION

A. Actinometry

Some of the species that are expected to play an important role in the film deposition (H, CH) were easily observed in the discharge. Table I lists the species of interest, the wavelength, and the respective excitation thresholds.

We used the nitrogen and argon actinometers which gave some indication of the behavior of the electron energy distribution as a function of a plasma parameter, in this case the pressure of acetylene.

The intensity of the light emitted by any chemical species x whose excitation resulted directly from electronic impact and whose de-excitation occurred by one photon emission is given by

$$I_x = KN_x\eta_x = K'\eta_x \int_0^\infty \sigma(E)N_e(E)dE, \quad (3)$$

where N_x is the ground state concentration of the species, η_x is the excitation efficiency, and $N_e(E)dE = E^{1/2}F_e dE$ represents the number of electrons per unit volume of the plasma in the energy range dE . Here, F_e is the electron energy distribution function (EEDF), $\sigma(E)$ is the excitation cross sec-

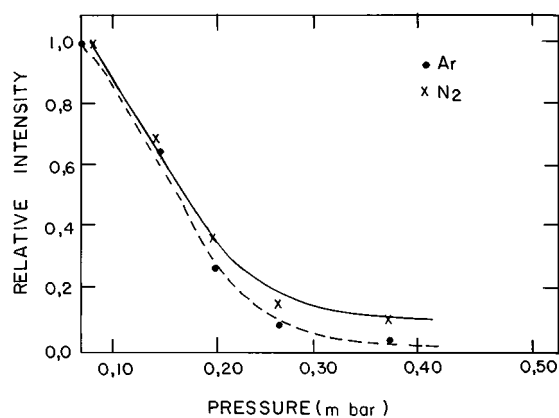


FIG. 1. Relative intensities of the actinometers argon and nitrogen measured as a function of the C₂H₂ pressure in discharges maintained at an applied rf power of 12 W.

tion to the state responsible for the emission, and K and K' are constants. Therefore it is apparent that, since the actinometer concentration remains constant in the discharge, variations in the emission intensity of the actinometer can be attributed to modifications in the EEDF. As the pressure of C₂H₂ changes, modification in both the plasma electron density and the average electron energy are to be expected, either of which will alter the EEDF. Thus, we propose, as previously,³¹ the use of a parameter A , defined as

$$A = \rho E, \quad (4)$$

where ρ is the mean electron density and E the mean electron energy. The parameter A therefore gives a rough indication of the *activity* of the plasma. Thus, by referring to this parameter, it is possible to avoid constant reference to an increase in the electron density or the electron mean temperature (or both).

Prior to each optical measurement or film deposition, the reactor was pumped down to 10^{-3} mbar. All the experiments were made at an applied rf power of 12 W and a flow rate of C₂H₂ in the range $0.68 \times 10^{-2} - 3.38 \times 10^{-2}$ Pa m³/s (1 Pa m³/s = 592 sccm), corresponding to an indicated pressure from 0.1 to 0.5 mbar. For these conditions, the nitrogen or argon actinometers were used at constant flow rate corresponding to 2% of the initial C₂H₂ pressure, i.e., 2% of 0.1 mbar during all of the experiments.

Figure 1 shows the light intensity emitted by the actinometers nitrogen and argon monitored as a function of the acetylene pressure in the discharge (the plots are normalized to one). Inspection of Fig. 1 shows that, for an increase in the C₂H₂ pressure, similar relative changes in the intensities of the two actinometers are observed. The similarity in the intensity curves of Ar and N₂ implies a similar influence of the increased C₂H₂ pressure on electrons of different energy.

To obtain trends in the relative concentration of the CH species we have normalized its optical emission intensity to that of the nitrogen line and to that of argon (spectral data are given in Table I). Although the threshold energy of N₂ to the state responsible for the transition measured here (11.2 eV) is closer to that of the transition of CH (<11 eV) than that of

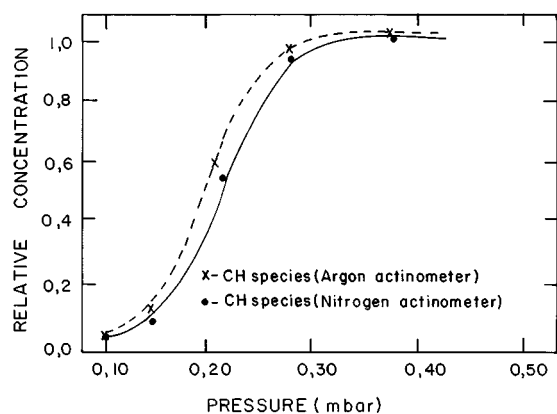


Fig. 2. Relative concentration of the CH species as a function of the C₂H₂ pressure at 12 W applied rf power (concentrations calculated using the actinometers Ar and N₂ are shown).

Ar (13.47 eV), the latter actinometer is preferable because Ar is an inert gas. In contrast, nitrogen is not only a diatomic molecule, but may also be incorporated into films deposited from plasmas of organic gases with nitrogen.

Figure 2 shows the trend in the concentration of CH in the plasma for experiments realized at pressures between 0.1 and 0.5 mbar, which are associated with different acetylene flow rates. A rapid increase is observed in the CH concentration in the discharge for pressures between 0.1 and 0.26 mbar and above this value the CH concentration remains fairly constant. This behavior may be considered the result of two competing factors, namely, the increase in the supply of C₂H₂ as the pressure is increased, and the simultaneous drop in the activity of the plasma. The first factor increases the supply of CH units; the second tends to reduce the degree of fragmentation.

It is clear from Fig. 2 that the choice of actinometer is not critical, but we prefer the use of Ar for the reasons already given above.

B. Infrared analysis

The films for analysis by infrared spectroscopy were grown at pressures of C₂H₂ between 0.1 and 0.5 mbar. Figure 3 shows an infrared spectrum characteristic of these films. The absorption bands due to C–H bonds are prominent in the spectrum of the film. The strong absorption at 2930 cm⁻¹ arises from symmetrical and asymmetrical stretching modes in CH₂ and CH₃ groups. Asymmetrical and symmetrical bending modes in CH₃ groups give rise to the bands at 1440 and 1375 cm⁻¹, respectively. Other absorptions are due to C=C (1624 cm⁻¹), carbonyl (1700 cm⁻¹), and hydroxyl (3500 cm⁻¹) groups. The last of these appears as a consequence of oxygen contamination, which may result from reactions with oxygen from water vapor or other oxygen-containing molecules still present in the reactor during film formation. It should be noted that the plasma polymers may contain a high concentration of free radicals, captured from the plasma.³² Thus, hydroxyl groups could arise from reactions between free radicals and the surrounding free oxygen.³³

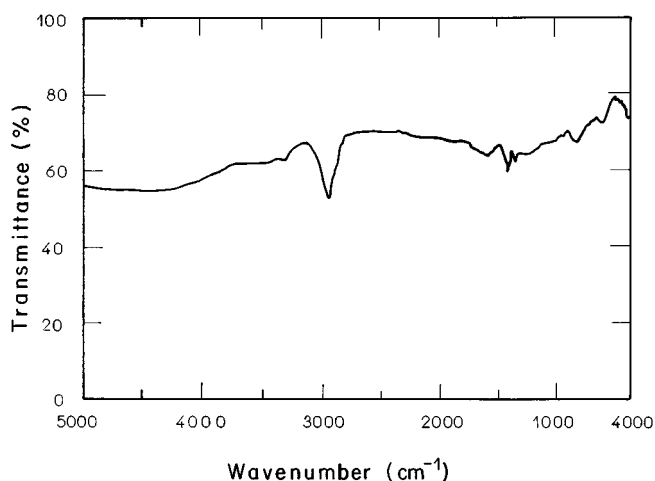


Fig. 3. Infrared spectrum of a typical plasma polymerized acetylene film. The discharge parameters were pressure =0.2 mbar and applied rf power=12 W. The film thickness was 6000 Å.

A quantitative evaluation of the relative C–H bond density can be made by calculation of the integrated absorption of the band at 2930 cm⁻¹. Figure 4 shows the integrated absorption of the C–H bond calculated by the method of Lanford and Rand³⁴ as a function of the C₂H₂ pressure in the discharge when the films were deposited. The increase in the C–H bond density is due to structural modification within the films. As a matter of fact, the power supplied to the discharge for a given pressure influences the deposition process, so that the increase in pressure results in greater quantities of CH in the plasma available for polymer deposition.

C. Correlation between deposition rate, IR analysis, and actinometry

Here, we discuss the correlation between the plasma CH concentration, the quantity of hydrogen in the polymer (C–H density) and the deposition rate of the film. The data of Figs. 2 and 4 show a strong correlation between the CH concen-

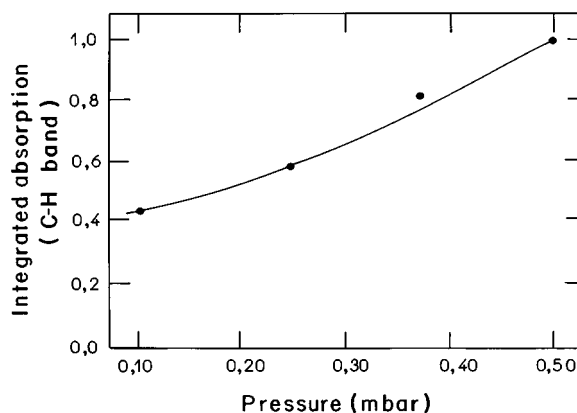


Fig. 4. Integrated absorption of the C–H band at 2930 cm⁻¹ as a function of pressure used for the deposition. Films were prepared from acetylene at an applied rf power of 12 W.

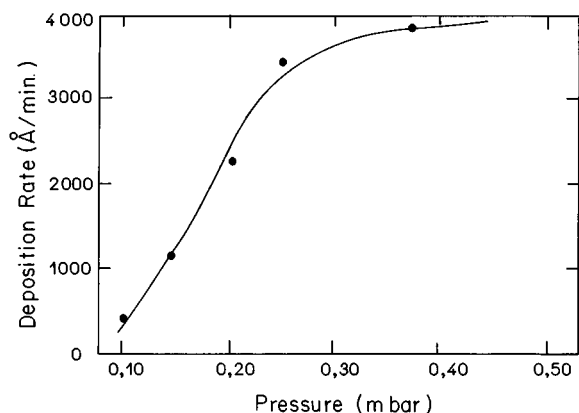


FIG. 5. Deposition rate of the plasma polymerized acetylene films as a function of the acetylene pressure at an applied rf power of 12 W.

tration in the plasma and the quantity of hydrogen in the polymer film. Both increase when the operating pressure of the system is increased.

Figure 5 shows the deposition rate of the plasma polymer films obtained as a function of C₂H₂ pressure in the system. It should be noted that the polymerization rate increases by a factor of 9 when the C₂H₂ pressure increases from 0.10 to 0.37 mbar.

To interpret these results we should remember that the electrons in the plasma are responsible for C₂H₂ fragmentation, thus producing many species in the discharge. The polymer deposition rate shows a very similar dependence on pressure as does the plasma CH concentration, independent of whether Ar or N₂ is used as the actinometer. This strongly suggests that the CH species in the plasma is one of the main precursors of polymer formation. This is in close agreement with the fact that higher concentrations of CH correspond to higher deposition rates of the polymer. In other words, these results are strongly indicative that the CH species is an elementary unit in the film formation process.

D. Optical properties

The refractive index and the optical absorption coefficient have been determined for various samples deposited from plasmas in acetylene. Using data from UV-visible transmission spectra, values of the refractive index for a photon energy of 1.25 eV were determined by a procedure described by Cisneros *et al.*³⁵ and are plotted in Fig. 6 as a function of the C₂H₂ pressure. The refractive index monotonically decreases from 1.74 to 1.63 as the pressure of the deposition increases from 0.1 to 0.5 mbar. The decrease in the refractive index can be attributed to the structural modification of the polymers with different quantities of hydrogen, and these values lie in the range 1.6–2.0 obtained for plasma polymerized C₂H₂ films by other authors.³⁶

For the computation of the optical transmission, the following equation was used

$$T = Ax / (Bx^2 + Cx + D), \quad (5)$$

where $x = \exp(\alpha d)$, α and d are the absorption coefficient and the thickness of the film, respectively. A , B , C , and D

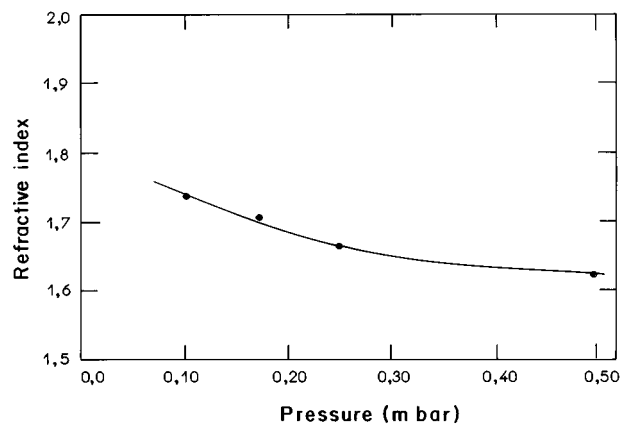


FIG. 6. The refractive index calculated at a photon energy of 1.25 eV for plasma polymerized acetylene films deposited at different pressures from 0.1 to 0.5 mbar at an applied rf power of 12 W.

are functions of the optical properties of the film and substrate.³⁷ Equation (5) was obtained from an expression given by Knittl³⁸ for a thin film deposited onto a weakly absorbing substrate.

Figure 7 illustrates the dependence of the optical absorption coefficient on the photon energy for various polymer films. In all the samples α rises sharply, showing an absorption edge similar to other materials such as amorphous hydrogenated carbon.³⁹ Differences in the optical absorptions of materials can be characterized by an optical gap. In our polymer films we defined as an optical gap, the photon energy $E_{0.4}$ corresponding to the absorption at $\alpha = 10^4 \text{ cm}^{-1}$, as

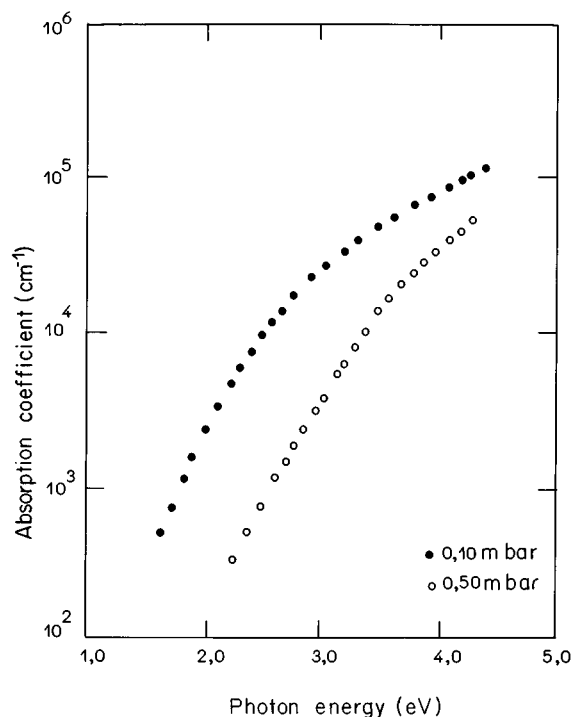


FIG. 7. The optical absorption coefficient of the plasma polymerized acetylene films calculated as a function of the photon energy.

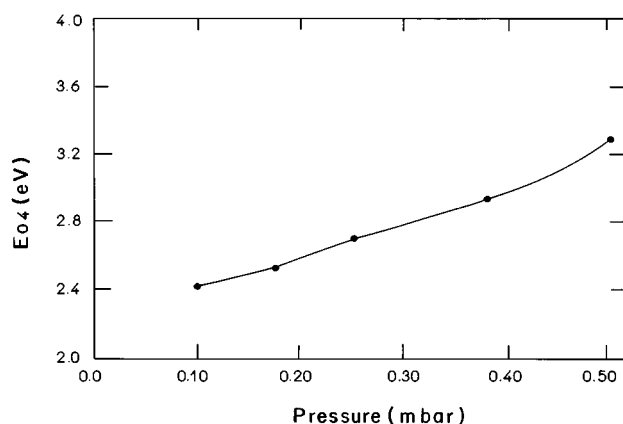


FIG. 8. The optical gap E_{04} of the plasma polymerized films as a function of acetylene pressure used for the deposition (applied rf power = 12 W.)

Freeman and Paul⁴⁰ have used to characterize the absorption edge of amorphous semiconductors.

Figure 8 shows a plot of values of the optical gap E_{04} as a function of the C₂H₂ pressure in the plasma deposition, obtained from the absorption curves like those of Fig. 7. The values of E_{04} increase as the pressure is increased in the range of 0.1–0.5 mbar. As shown in Fig. 4, the C–H bond density (quantity of hydrogen) in the sample prepared at 0.5 mbar is 2.3 times higher than the quantity of hydrogen in the sample deposited at 0.1 mbar. Thus, we can see that an increase in film hydrogen concentration can cause an increase in the optical gap of these polymers. It should be remembered that in many amorphous materials absorption can be described by the well-known Tauc model⁴¹ according to which

$$(\alpha E)^{1/2} = \beta(E - E_g), \quad (6)$$

where E_g is the optical gap and β is a constant. Since the optical data of our samples did not reveal a linear relationship between $(\alpha E)^{1/2}$ and E , the optical gap could not be determined by Eq. (6).

The random structure of the carbon chains in a plasma polymer makes theoretical interpretation of the experimental results rather difficult. However, it seems reasonable to suppose that some trends in the physical behavior of a *conventional* polymer must be followed by a plasma polymer. In conjugated polymers, for instance, the π bonds play a very important role in the electronic conduction, affecting the density of the states and the band gap. The density of π bonds is influenced by the hydrogen content. Hydrogen forms σ bonds with the carbon atoms at the expense of the π bonds. It may be noted that the attachment of hydrogen to the polymer affects bonds lengths, thus changing the band gap.

E. Residual stress measurements

The evolution of the residual stress as a function of film thickness for various plasma polymerized acetylene films is shown in Fig. 9. Each curve was obtained at a different discharge pressure. The values of the residual stress for the

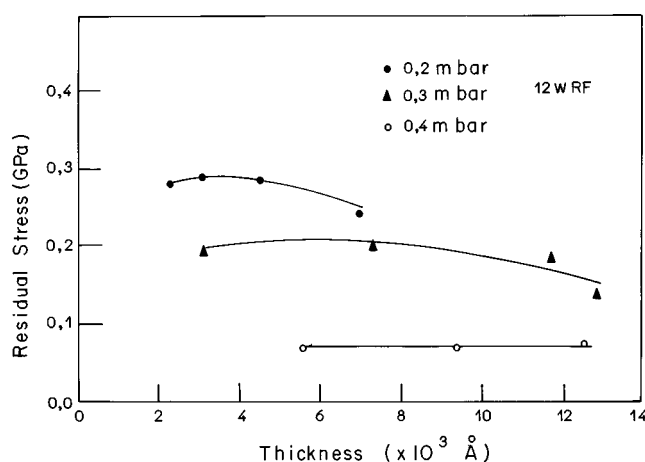


FIG. 9. Residual stress as a function of film thickness for the plasma polymerized acetylene films prepared at an applied rf power of 12 W.

films deposited at 0.2 mbar increase with the thickness in the interval of 2000–3000 \AA and decrease between 3000 and 7000 \AA . The stress in the film prepared at 0.3 mbar increases between 3000 and 7000 \AA , decreasing thereafter. The values of the residual stress for polymers obtained at 0.4 mbar remain approximately constant between 5500 and 12 000 \AA . Comparing the three curves in the interval 3000–7000 \AA , we observe that at a constant thickness the stress decreases with increasing pressure. This behavior is also indicated by the curves corresponding to the films deposited at 0.3 and 0.4 mbar in the interval of thickness between 7000 and 12 000 \AA . Thus, films of the same thickness obtained at high pressure will be less stressed than those obtained at low pressure.

On the other hand, it is interesting to observe that the deposition rate of the polymers increases when the pressure increases, as shown in Fig. 5. So the residual stress decreases whereas the deposition rate increases. One possible explanation of this fact is that by increasing the pressure, the number of collisions between the reactive species of the gaseous phase increases too, because the mean free path decreases; consequently the chemical reaction rate will increase, increasing the polymerization rate. Plasma polymerization results in polymers which are products of the linking of *blocks* by the so-called *growth chain mechanism* described by Yasuda.⁴² The blocks are short carbon chains containing (or not) free radicals produced in the plasma when the acetylene molecule is broken. The successive building of these blocks produces an expansive effect in the film that is known as the *wedge effect*. This causes a compressive residual stress in the polymer film. Increasing the polymerization rate, the length of the blocks increases. The deposition of greater blocks decreases the wedge effect and consequently decreases the value of the residual stress in the films. When polymer films are deposited at low pressure, the mean free path is smaller than that of the initial situation (high pressure). So, the polymerization rate decreases because the reaction rate decreases in the gaseous phase. Therefore, blocks with smaller length will be deposited, increasing the wedge effect, and the residual stress value will be increased.

IV. CONCLUSIONS

Actinometric optical emission spectrometry measurements of film-depositing rf discharges of C₂H₂ revealed that the plasma activity falls as the system pressure increased. Analysis of the molecular structure of the thin films showed that hydrogen concentrations in the samples also depend on the pressure of C₂H₂. The concentration of hydrogen increases when the pressure is increased. The deposition rate of the films is correlated with the concentration of CH species in the discharge and we concluded that the CH species constitute an elementary block in the plasma polymerization of acetylene. Modifications in the chemical structure of polymers prepared in rf discharges due to the increase in the hydrogen levels in these polymers can change the refractive index and the optical gap of these materials. The refractive index decreases with the increase in the hydrogen concentration of the films, while the optical gap increases. Hydrogen forms σ bonds with the carbon atoms at the expense of π bonds. At the same time, the attachment of hydrogen to the polymer affects bond lengths, thus changing the band gap. As previously observed, the residual stress depends on the thickness and the structural composition of the polymer films. Therefore, we can suppose that during the growth of the polymer, the wedge effect occurs due to the atomic packing, which produces compressive stress.

ACKNOWLEDGMENTS

The authors thank CNPq, FAPESP, and FUNDUNESP for financial support. They are also grateful to Geraldo F. Gomes and Professor Dr. Maurício A. Algatti for valuable discussions and Carlos S. Lambert for technical assistance.

¹J. Goodman, *J. Polym. Sci.* **44**, 551 (1960).

²Y. Osada and M. Takase, *J. Polym. Sci.: Polym. Chem.* **23**, 2425 (1985).

³J. L. Gittleman, B. Abeles, and A. Rose, *Phys. Rev. Lett.* **27**, 19 (1975).

⁴H. G. Craighead, R. Bartinski, R. A. Buhrman, L. Wojcik, and J. Siexies, *Sol. Energy Mater.* **1**, 105 (1979).

⁵T. Kashiwagi, K. Okabe, and K. Okita, *J. Membr. Sci.* **36**, 353 (1988).

⁶F. G. Yamagishi, D. D. Grangen, A. E. Shimitz, and L. J. Miller, *Thin Solid Films* **24**, 427 (1981).

⁷I. R. Hollagan, T. Wydeven, and C. C. Johnson, *Appl. Opt.* **13**, 1844 (1974).

⁸P. Schreiber, M. R. Wertheimer, and A. M. Wrobel, *Thin Solid Films* **72**, 487 (1980).

⁹N. Inagaki, K. Suzuki, and K. Nejigaki, *J. Polym., Polym. Lett.* **21**, 353 (1983).

¹⁰E. J. Hsieh and R. Y. Shineda, *Solid-State Electron* **12**, 493 (1969).

¹¹M. Hori, H. Yamada, T. Yoneda, S. Morita, and S. Hattori, *J. Electrochem. Soc.* **134**, 707 (1987).

¹²M. Hori, H. Yamada, T. Yoneda, S. Morita, and S. Hattori, *J. Electrochem. Soc.* **135**, 2649 (1988).

¹³H. Yamada, J. Tamano, T. Yoneda, S. Morita, and S. Hattori, *Jpn. J. Appl. Phys.* **21**, 768 (1982).

¹⁴P. K. Tien, G. R. Smolinski, and R. J. Martin, *Appl. Opt.* **11**, 637 (1972).

¹⁵N. P. Cheremisinoff, *J. Miner.* **42**, 10 (1990).

¹⁶H. Yasuda, *J. Polym. Sci. Macromol. Rev.* **16**, 199 (1981).

¹⁷T. Shiosawa, M. A. Bica de Moraes, and J. Scarminio, *J. Appl. Phys.* **70**, 4888 (1991).

¹⁸D. R. McKenzie and L. M. Briggs, *Sol. Energy Mater.* **6**, 97 (1981).

¹⁹S. Craig and G. L. Harding, *Thin Solid Films* **97**, 345 (1982).

²⁰B. Abeles, P. Sheng, M. D. Coutts, and Y. Arie, *Thin Solid Films* **24**, 407 (1975).

²¹R. M. Hill and T. J. Coutts, *Thin Solid Films* **42**, 201 (1977).

²²P. Couderc and V. Catherine, *Thin Solid Films* **146**, 93 (1987).

²³T. Frauenheim, U. Stephan, K. Bevilaqua, F. Janquickel, P. Blaudeck, and F. Fromn, *Thin Solid Films* **182**, 63 (1989).

²⁴H. C. Tsai and D. B. Bogy, *J. Vac. Sci. Technol. A* **5**, 63 (1989).

²⁵J. W. Coburn and M. Chen, *J. Appl. Phys.* **51**, 3134 (1980).

²⁶R. d'Agostino, L. Martinu, and V. Pische, *Plasma Chem. Plasma Process* **11**, 243 (1991).

²⁷R. A. Gottscho and T. A. Miller, *Pure and Appl. Chem.* **56**, 189 (1984).

²⁸R. P. Mota, Ph.D. thesis, IFGW/UNICAMP, Brazil, 1992.

²⁹M. Tong and K. L. Saenger, *J. Appl. Phys. Sci.* **38**, 937 (1989).

³⁰T. Shiosawa, M.S. thesis, IFGW/UNICAMP, Brazil, 1991.

³¹S. F. Durrant, R. P. Mota, and M. A. B. de Moraes, *Thin Solid Films* **220**, 295 (1992).

³²N. Morosoff, B. Crist, M. Bumgarner, T. Hsu, and H. Yasuda, *J. Macromol. Sci. Chem. A* **10**, 451 (1976).

³³H. Yasuda, M. O. Bumgarner, H. C. Marsh, and N. Morosoff, *J. Polym. Sci. Polym. Chem.* **14**, 195 (1976).

³⁴W. A. Lanford and M. J. Rand, *J. Appl. Phys.* **49**, 2473 (1988).

³⁵J. I. Cisneros, G. B. Rego, M. Tomyiama, S. Bilac, J. M. Gonçalves, A. E. Rodrigues, and Z. P. Arguello, *Thin Solid Films* **100**, 155 (1983).

³⁶D. R. McKenzie, R. C. McPhedran, and N. Savvides, *Philos. Mag.* **48**, 341 (1983).

³⁷S. F. Durrant, R. P. Mota, and M. A. B. de Moraes, *J. Appl. Phys.* **71**, 448 (1992).

³⁸Z. Knittel, *Optics of Thin Films* (Wiley, New York, 1976).

³⁹W. Smith, *J. Appl. Phys.* **55**, 764 (1984).

⁴⁰E. C. Freeman and W. Paul, *Phys. Rev. B* **20**, 716 (1979).

⁴¹J. Tauc, *Optical Properties of Solids*, edited by F. Abeles (North-Holland, Amsterdam, 1972), Chap. 5.

⁴²H. Yasuda, *Plasma Polymerization* (Academic, Orlando, 1985), Chap. 6.